

LETTER

Measurement and Evaluation of the Bioelectrical Impedance of the Human Body by Deconvolution of a Square Wave

Yuhwai TSENG^{†a)}, Chauchin SU^{††}, *Nonmembers*, and Chien-Nan Jimmy LIU[†], *Member*

SUMMARY In this study, we use the deconvolution of a square test stimulus to replace a series of sinusoidal test waveforms with different frequencies to simplify the measurement of human body impedance. The average biological impedance of body parts is evaluated by constructing a frequency response of the equivalent human body system. Only two stainless-steel electrodes are employed in the measurement and evaluation.

key words: *body impedance, square test waveform, deconvolution*

1. Introduction

The electrical impedance of body parts significantly affects the techniques for the measurement of physiological events and the investigation of tissue structures such as *Electroencephalography* (EEG), *Electrocardiography* (ECG), *Electromyography* (EMG), *Electronystagmography* (ENG), impedance cardiography, and electrical impedance tomography. Understanding the impedance characteristic of body parts has received considerable attention recently, especially for the development of a wideband *intra-body communication* (IBC) system ([1], [2]) in which the human body functions as a transmission medium to integrate electronic products discretely located in individuals such as mobile and ear phones, PDAs, wearable personal computers, as well as biomedical sensors and actuators. Elucidating the average electrical impedance of human body parts in the frequency band below several tens of megahertz facilitates the design of medical instruments and a wideband IBC system, which will ultimately benefit users of electronic equipment.

Conventional methods of measuring the bioelectric impedance of the human body are divided into two categories. Methods in one category measure the impedance of skin and body parts using a series of sinusoidal test waveforms with various frequency inputs into the measured human body; the bioelectrical impedance of the human body is then evaluated using the output voltage and current of the measured human body ([3]–[7]). The methods in the other category input a square waveform into the measured human body to differentiate the transient response of the resulting current in order to estimate bioelectrical impedance

([8]–[10]).

In this study, we describe a simplified model of the human body made from living tissues of body parts. Based on the deconvolution of a square test waveform, the frequency responses of the high-pass and low-pass systems of the human body are constructed and the measurement procedures are simplified as well. Then, the average bioelectric impedance of the human body is determined in a straightforward manner.

2. Materials and Methods

2.1 Model of the Human Body System

Figure 1 shows a simplified human body system designed by applying an equivalent circuit model of the skin and body impedance. The human body is modeled as a simplified circuit consisting of the skin resistances R_{X1} and R_{X2} , the skin capacitances C_{X1} and C_{X2} , and body impedance; it is composed of living tissues of body parts ([11], [12]). R_e is the resistance of extracellular fluid. C_m and R_m are the membrane capacitance and intracellular fluid resistance of muscle tissues, respectively. C_b and R_b represent the membrane capacitance and intracellular fluid resistance of red blood cells, respectively. C_t is the capacitance of tissues of body parts. Notably, C_B represents the capacitor between the body and

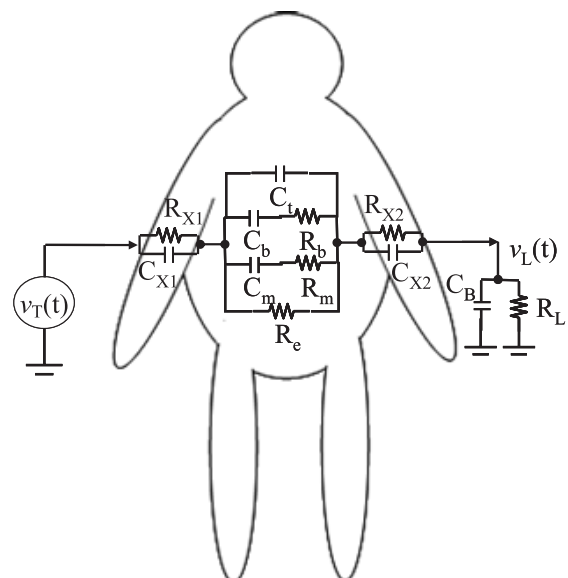


Fig. 1 Simplified equivalent circuit model of the human body.

Manuscript received October 26, 2009.

Manuscript revised January 29, 2010.

[†]The authors are with the Electrical Engineering Department, National Central University, No. 300, Jung-Da Rd., Jhong-Li City Taiwan 320, R.O.C.

^{††}The author is with the Department of Electrical and Control Engineering, National ChiaoTung University, No. 1001, Ta-Hsueh Rd., Hsin-Chu City, Taiwan 300, R.O.C.

a) E-mail: s0541004@cc.ncu.edu.tw

DOI: 10.1587/transinf.E93.D.1656

the ground. In this study, we add a test signal $v_T(t)$ and a load resistance R_L on both sides of the body; additionally, $v_L(t)$ is the voltage across the load resistance R_L . We assume that $R_{X1} = R_{X2} = R_X$ and $C_{X1} = C_{X2} = C_X$. The typical R_X of dry skin is in the range of several hundreds of $k\Omega$, and C_X is in the range of several tens of nf . $R_X \gg X_{C_X}$ (where $X_{C_X} = \left| \frac{1}{sC_X} \right|$). Accordingly, the contribution of the skin resistance R_X is neglected. Various load resistances can transform the system into a high- or low-pass system. Skin and body impedances are estimated in a specified frequency range.

2.2 High-Pass System for Determining Body Part Impedance and Skin Capacitance

A specific frequency band and the load resistance R_L are selected, such that $X_{CB} \gg R_L$ (where $X_{CB} = \left| \frac{1}{sC_B} \right|$ and C_B is typically in the range of several tens of pF). Thus, C_m , R_m , C_b , R_b , C_t and C_B can be eliminated from Fig. 1. Figure 1 becomes a simplified high-pass system with transfer function

$$|H(s)| \cong \frac{R_L}{R_e + R_L + \left| \frac{1}{sC_X} \right|}. \quad (1)$$

When R_L and the measured $|H(s)|$ are known, R_e and C_X are derived from Eq. (1) by interpolation from the measured $|H(s)|$ versus frequency. Then, after a frequency band is selected and C_b , R_b , C_t and C_B are eliminated, Eq. (1) becomes

$$|H(s)| \cong \frac{R_L}{R_e \parallel \left(R_m + \left| \frac{1}{sC_m} \right| \right) + R_L + \left| \frac{1}{sC_X} \right|}. \quad (2)$$

With knowledge of R_e and C_X , R_m and C_m can be similarly determined.

Next, R_b is eliminated by selecting a specific frequency band, which allows $\left| \frac{1}{sC_b} \right| \gg R_b$. Equation (2) thus becomes

$$|H(s)| \cong \frac{R_L}{R_e \parallel \left(R_m + \left| \frac{1}{sC_m} \right| \right) \parallel \left| \frac{1}{s(C_b + C_t)} \right| + R_L + \left| \frac{1}{sC_X} \right|}. \quad (3)$$

$(C_b + C_t)$ is obtained using the method mentioned above. Then, increasing the test signal frequency band to several tens of megahertz transforms Eq. (3) into

$$|H(s)| \cong \frac{R_L}{R_B + R_L + \left| \frac{1}{sC_X} \right|}. \quad (4)$$

where R_B denotes $R_e \parallel \left(R_m + \left| \frac{1}{sC_m} \right| \right) \parallel \left(R_b + \left| \frac{1}{sC_b} \right| \right) \parallel \left| \frac{1}{sC_t} \right|$. Since $2\pi f R_b C_b \gg 1$ under a specific test frequency band, R_b is eliminated from Eq. (4); in addition, C_b and C_t are obtained from Eqs. (3) and (4), respectively. Finally, by selecting a reasonable test frequency band and with knowledge of R_e , C_X , R_m , C_m , C_b , and C_t , R_b is derived from Eq. (4).

2.3 Low-Pass System for Determining C_B

Similarly, a specific frequency range and the load resistance R_L can be derived such that $X_{CB} \ll R_L$. The system model then becomes a low-pass system. C_B is derived as

$$C_B \cong \frac{1}{\omega \times |V_L(s)|} \times \left[\frac{|V_T(s)|}{R_B} - \frac{|V_L(s)|}{R_L \parallel R_B} \right]. \quad (5)$$

2.4 Deconvolution on Square Test Stimulus

A square waveform consists of multiple odd harmonics that facilitates the acquisition of information in an expanded frequency range within a single measurement. The amplitude of the n^{th} harmonic of a square waveform with amplitude A , and 50% duty cycle can be represented as

$$|V(n)| = \frac{A}{n\pi} \quad n = 1, 3, 5, 7, \dots \quad (6)$$

The output signal $v_L(t)$ of the system shown in Fig. 1 is a convolution operation of the input signal $v_T(t)$ and the system impulse response $h(t)$.

$$v_L(t) = v_T(t) \otimes h(t). \quad (7)$$

In the frequency domain, the output is the product of the input and the transfer function. With the circuit model shown in Fig. 1, the output is

$$V_L(s) = V_T(s) \times H(s). \quad (8)$$

To obtain the system transfer function $H(s)$, the output $V_L(s)$ is divided by the input $V_T(s)$. Such an operation in the time domain is called deconvolution [13].

3. Experimental Setup

The measurement evaluates the bioelectrical impedance of body parts from the left wrist to either the left arm 40 cm away or the right wrist 1.5 m away from the left wrist. The measured human body is that of a male 1.75 m in height and 70 kg in weight.

Figure 2 shows the experimental setup. An Agilent 33250A wave generator and an Agilent 54382D oscilloscope were employed to generate and receive the test square stimulus, respectively. In the measurement, we apply two stainless-steel electrodes with a surface area of 6 cm^2 to connect the measured human body directly to the waveform generator and oscilloscope. The test stimulus is a $\pm 1 \text{ V}$ square wave with a 50% duty cycle. The Matlab tool is utilized to transfer the stimulus signals $v_T(t)$ and the body output signals $v_L(t)$ from the time domain to the frequency domain $V_T(s)$ and $V_L(s)$. Then, the deconvolution of $V_L(s)$ by $V_T(s)$ is performed to obtain the system transfer function $H(s)$ in Eq. (8).

On the basis of Eq. (1)–(5), 5 and 100 kHz square waves with load resistances R_L of 25Ω and $10 \text{ k}\Omega$ are

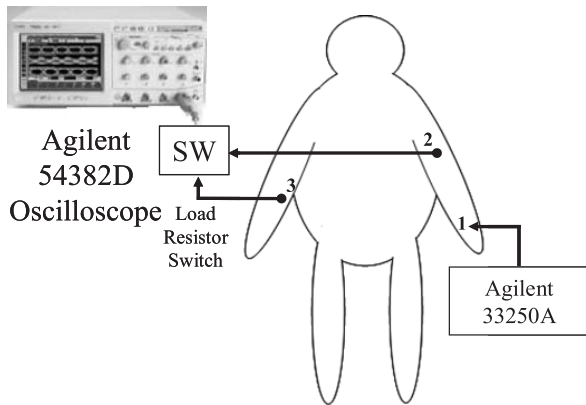


Fig. 2 Block diagram of experimental setup.

selected to construct the frequency response of a high-pass (frequency range from 5 kHz to 3.5 MHz with spacing frequency 10 kHz) and low-pass (frequency range from 100 kHz to 8.3 MHz with a spacing frequency of 200 kHz) systems of the human body to evaluate the body part impedance, respectively. To obtain C_b and C_t , a 2 MHz square wave with R_L of 25Ω is selected to realize a high-pass system for the human body with a frequency rang from 18 MHz to 24 MHz and a spacing frequency of 4 MHz.

4. Results and Discussion

Figure 3 and Table 1 show a summary of the evaluation results of the average bioelectric impedance of related body parts from the left wrist to the left arm and right wrist versus a specified frequency range. Due to the circuit approximation and simplification of Fig. 1 and Eq. (1)–(5), the evaluation results except C_x and R_e vary slightly and approximate to a constant in a specific frequency range. Table 1 shows a list of the measurement parameters and values of the evaluation results. Figure 3 (c) reveals that when the specified frequency is > 15 kHz, the evaluation results of the R_e do not approximate a constant since a series combination of reactance C_m and resistance R_m is no longer larger than R_e ; in addition, C_m and R_m cannot be eliminated. The specified frequency range of C_x and R_e is below 15 kHz.

Evaluation results indicate that the R_e , R_m , and R_b of body parts are proportional to the distance between the measurement point and the cross-sectional area covered by the measured body. Components of the upper body consist mainly of a chest cavity in which the main direction of blood flow in the main blood vessel is longitudinal, explaining why R_b evaluated from the transverse direction of the upper body is eight times higher than R_b from the longitudinal direction of only the right or the left arm. Additionally, C_m , C_b , C_t , and C_B are inversely proportional to the distance between the measurement points. The skin capacitance C_x evaluated at the right arm is the same as the value evaluated at the left wrist.

The equivalent circuit model of the simplified human body system shown in Fig. 1 and the related parameters in

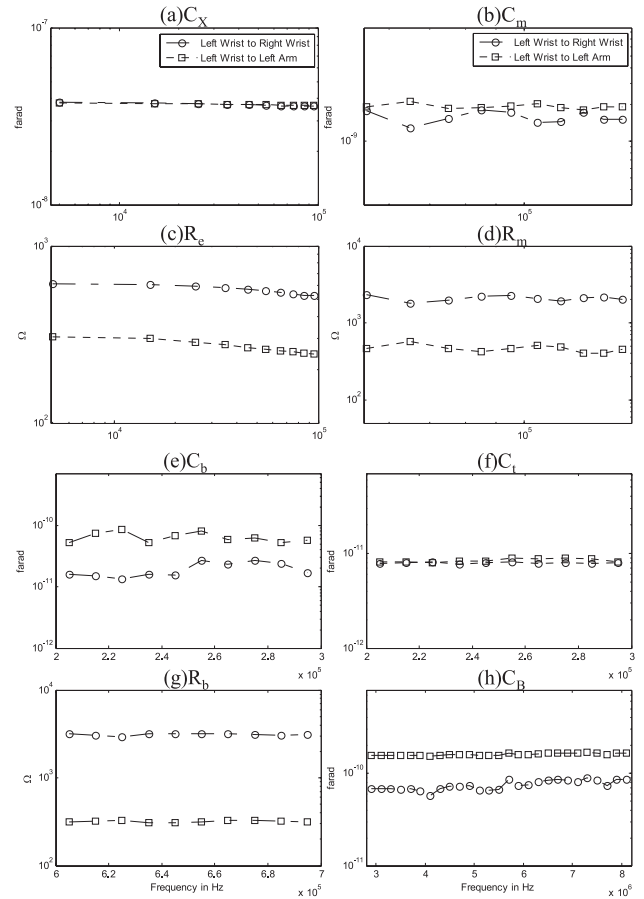


Fig. 3 Evaluation results of bioelectric impedance of body parts (a) Skin capacitance. (b) Membrane capacitance of muscle tissues. (c) Resistance of extracellular fluid. (d) Intracellular fluid resistance of muscle tissues. (e) Membrane capacitance of red blood cells. (f) Capacitance of tissue of the body parts. (g) Intracellular fluid resistance of red blood cells. (h) Capacitance between the body and the ground.

Table 1 Evaluation results of average bioelectric impedance of body parts and corresponding measurement parameters.

	R_L (Ω)	Specific Frequency Range	Test Square Wave	Left Wrist To		
				Left Arm	Right Wrist	
C_x	25	5kHz	5 kHz	38nF	38nF	
R_e				305 Ω	613 Ω	
C_m		55kHz~145kHz		1.93nF	1.58nF	
R_m				462 Ω	2.05k Ω	
C_b		205kHz~295kHz		5 kHz	65pF	19pF
C_t		18MHz~24MHz		2 MHz	8.4pF	7.9pF
R_b		605kHz~695kHz		5 kHz	320 Ω	3.12k Ω
C_B		10k		3MHz~7MHz	100 kHz	161pF

Table 1 are simulated using the Hspice circuit simulator. To verify the accuracy of the body impedance measurement by deconvolution of a square test waveform, in this work, we compare the results obtained using the Hspice circuit simulator and the proposed measuring method. Three male subjects were evaluated in the verification procedures with their

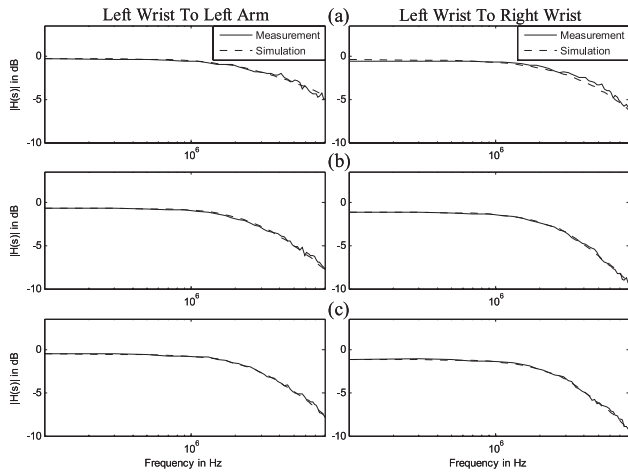


Fig. 4 Results of simulation and proposed evaluation method for simplified low-pass system: (a) Subject A, (b) Subject B, and (c) Subject C.

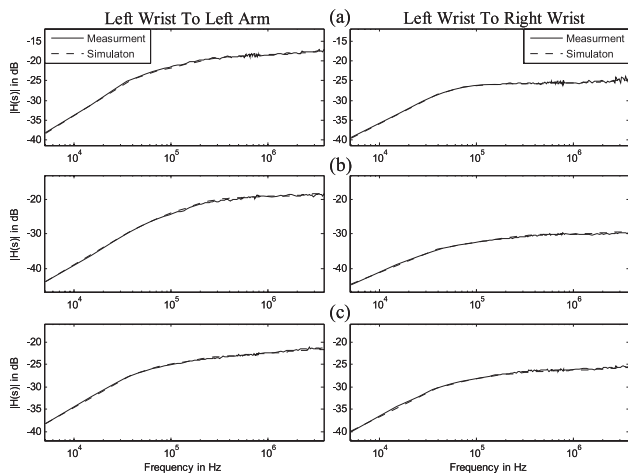


Fig. 5 Results of simulation and proposed evaluation method for simplified high-pass system: (a) Subject A, (b) Subject B, and (c) Subject C.

ages ranging from 24 to 45 years old, heights ranging from 1.64 to 1.8 m, and weights ranging from 66 to 82 kg. Figures 4 and 5 show a summary of the results of the simulation and the proposed evaluating method from the left wrist to the left arm and right wrist. According to the figures, the simulation results closely resemble the measurement results. The maximum difference between the simulation and measurement results is < 0.2 dB, with a system relative error less than 2.3%.

Each of the evaluated average body impedances in Table 1 is manipulated separately with a variation of $\pm 10\%$ to calculate system relative error. Table 2 shows the calculation results with the corresponding maximum errors. The maximum system relative error of 2.8% occurs when R_e (from left wrist to left arm) decreases by 10% under the condition of the low-pass system. The accuracy is sufficient for evaluating the average electrical impedance of human body parts under a maximum measurement frequency of 8.3 MHz.

Table 2 Calculated system relative errors.

		Left Wrist To Left Arm								
Variation Rate	Variable	C_x	R_e	C_m	R_m	C_b	R_b	C_t	C_B	
	+10%	High Pass	0.02%	0.11%	0.11%	0.57%	0.01%	0.11%	0.11%	0.8%
Low Pass		0.01%	1%	1.7%	0.8%	1.3%	1%	0.9%	0.8%	
-10%	High Pass	0.5%	0.1%	0.1%	0.5%	0.02%	0.1%	0.1%	0.1%	
	Low Pass	0.01%	2.8%	0.9%	1%	1.5%	0.9%	0.1%	2.4%	
		Left Wrist To Right Wrist								
+10%	High Pass	0.02%	0.85%	0.97%	0.51%	0.09%	1%	1%	1%	
	Low Pass	0.01%	1.1%	2%	1.9%	2.2%	2.2%	1.2%	0.2%	
-10%	High Pass	0.5%	1%	0.9%	0.5%	0.9%	1%	1%	1%	
	Low Pass	0.01%	1.4%	2.1%	1.6%	2.2%	0.9%	1.2%	0.2%	

5. Conclusions

In this study, we utilize the deconvolution of square test waves to simplify the measurement procedure of human body impedance. By properly selecting load resistance and test square signal frequency, the band-pass system of the human body can be transformed into a high- or low-pass system; in addition, the average bioelectric impedance of the human body can be determined straightforwardly. The reliability of the proposed evaluation method is verified by deconvoluting square waves of 5 kHz and 100 kHz with load resistances R_L of 25 Ω and 10 k Ω , respectively. Results of this study demonstrate that the proposed evaluation method differs from practical measurements and simulation by less than 0.25 dB and a maximum relative error of 2.8% under a maximum measurement frequency of 8.3 MHz.

Acknowledgments

The authors would like to thank the National Science Council of the Republic of China, Taiwan, for financially supporting this research.

References

- [1] T.G. Zimmerman, "Personal area network: Near-field intrabody communication," IBM Syst. J., vol.35, no.3&4, pp.609–617, 1996.
- [2] Y. Tseng, C. Su, and CN.J. Liu, "Analysis and design of wide-band digital transmission in an electrostatic-coupling intra-body communication system," IEICE Trans. Commun., vol.E92-B, no.11, pp.3557–3563, Nov. 2009.
- [3] J. Rosell, J. Colominas, P. Riu, R. Pallas, and J.G. Webster, "Skin impedance from 1 Hz to 1 MHz," IEEE Trans. Biomed. Eng., vol.35, no.8, pp.649–651, Aug. 1988.
- [4] D. Panescu, K.P. Cohen, J.G. Webster, and R.A. Stratbucker, "The mosaic electrical characteristics of the skin," IEEE Trans. Biomed. Eng., vol.40, no.5, pp.434–439, May 1993.
- [5] R.P. Areny and J.G. Webster, "Bioelectric impedance measurements using synchronous sampling," IEEE Trans. Biomed. Eng., vol.40, no.8, pp.824–829, Aug. 1993.
- [6] Y. Yamamoto and T. Nakamura, "Consideration of conditions required for multi-channel simultaneous bioimpedance measurement," IEEE Instrumentation and Measurement Technology Conference, pp.18–20, St. Paul, Minesota, USA, May, 1996.
- [7] J.J. Huang, K.S. Cheng, and C.J. Peng, "Temperature-compensated

- bioimpedance system for estimating body composition," *IEEE Engineering in Medicine and Biology*, pp.66-73, Nov./Dec. 2000.
- [8] Y. Yamamoto, H. Isshiki, and T. Nakamura, "Instantaneous measurement of electrical parameters in a palm during electrodermal activity," *IEEE Trans. Instrumentation and Measurement. Eng.*, vol.45, no.2, pp.483-487, April 1996.
- [9] S.J. Dorgan and R.B. Reilly, "A model for human skin impedance during surface functional neuromuscular stimulation," *IEEE Trans. Rehabil. Eng.*, vol.7, no.3, pp.341-348, Sept. 1999.
- [10] A.F. Coston and J.K. Li, "Transdermal drug delivery: A comparative analysis of skin impedance models and parameters," *Proc. 25th Annual International Conference of IEEE EMBS*, pp.17-21, Cancun, Mexico, Sept. 2003.
- [11] H. Kanai, M. Haeno, and K. Sakamoto, "Electrical measurement of fluid distribution in legs and arms," *Med. Prog. Tech.*12: pp.159-170, 1987.
- [12] H. Kanai, I. Chatterjee, and O.P. Gandhi, "Human body impedance for electromagnetic hazard analysis in the VLF to MF band," *IEEE Trans. Microw. Theory Tech.*, vol.MTT-32, no.8, pp.763-771, Aug. 1984.
- [13] C. Su and Y.T. Chen, "Intrinsic response extraction for the removal of the parasitic effects in analog test buses," *IEEE Trans. Comput.-Aided Des. Integr. Circuits Syst.*, vol.19, no.4, pp.437-445, April 2000.
-